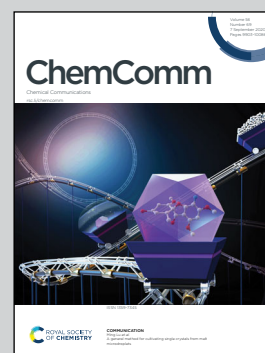**Showcasing research from Professor Takashi Kato's Group, Department of Chemistry and Biotechnology, School of Engineering, The University of Tokyo, Tokyo, Japan.**

Thermally tunable selective formation of self-assembled fibers into two orthogonal directions in oriented liquid-crystalline smectic templates

Fibrous assemblies of a gelator are formed into grid-like structures in liquid-crystalline smectic templates. The formation of these two orthogonal (grid-like) and one directional fibrous structures are selectively achieved by changing thermally tuned layered smectic structures.

As featured in:

See Takashi Kato *et al.*, *Chem. Commun.*, 2020, **56**, 9954.

ROYAL SOCIETY
OF **CHEMISTRY**

rsc.li/chemcomm

ROYAL SOCIETY
OF CHEMISTRY

Check for updates

Thermally tunable selective formation of self-assembled fibers into two orthogonal directions in oriented liquid-crystalline smectic templates†

Daisuke Yamaguchi, [ID][a] Yuka Ikemoto [ID][b] and Takashi Kato [ID]⋆[a]

We demonstrate the formation of grid-type (crossed perpendicular to each other) fibrous assemblies of low-molecular-weight gelators in aligned liquid-crystalline smectic templates. In the template of layered structures, a gelator forms oriented fibers with one directional and two orthogonal directional (grid-like) alignment depending on the order of layered structures.

One-dimensional self-assembly of organic gelators has received much attention as anisotropic functional materials.[1–7] Self-assembly of low-molecular-weight gelators in solution leads to the formation of randomly dispersed fibrous networks via non-covalent intermolecular interactions.[1–4] Functional fibrous assemblies have been developed in various fields including electrooptics,[8–10] regenerative medicine,[11,12] and stimuli-responsive materials.[13,14] For further functionalization, morphologies such as aligned structures of fibers are important.[15–22] Different biological activities,[15–17] mechanical properties[18,19] and optical functions[20–22] are dependent on the morphologies and alignment of the fibrous structures. Control of fibrous molecular assembled structures is of importance to obtain novel nanostructured materials. Alignment control of fibrous materials has been explored by using various alignment methods such as shear flow, electro-spinning, electric and magnetic fields.[23–27] However, these methods still have difficulties to construct more complex patterned fibrous structures on microscale.

It is of interest to use liquid crystals for templates of materials synthesis.[3,28–35] We have obtained liquid-crystalline (LC) gels by orthogonal molecular assembly of liquid crystals and low-molecular-weight gelators.[3] Anisotropic aggregation of gelators in LC templates results in macroscopic alignment of functional self-assembled fibers.[20–22,29,30,36–39] The LC fields

also allow the formation of complicated fibrous structures such as loop-like fibers[40] or gradually twisted aligned fibers.[20] Therefore, the self-assembled composites of liquid crystals and gelators are versatile and advantageous approaches for the construction of complex fibrous structures.

Aligned fibrous molecular assemblies are formed in smectic A phases.[3] In these templates, two types of fibers, aligned parallel (type I)[34] or perpendicular (type II)[38] to the molecular layers, were formed (Fig. 1). These different fiber orientations will be based on the two orthogonal orders of smectic A phases, that is, orientational order and layer order. In orthogonal ordered structures of smectic A phases, gelators have a potential to form aligned fibers along the layers and LC molecular orientation depending on the order of layered structures. If we could tune the layered structures of LC smectic templates, fibers oriented in two orthogonal directions, both parallel and perpendicular to the LC molecular orientation (type III), were expected to be obtained.

LC smectic structures have been studied as a function of temperature.[41–43] In previous reports, the order parameter of smectic A phases of alkoxy-cyanobiphenyls is increased as the temperature is decreased.[41–43] This observation shows that more ordered layered structures of smectic A phases are formed
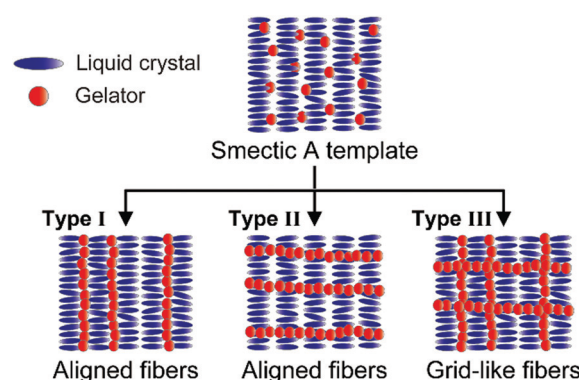
[a] Department of Chemistry and Biotechnology, School of Engineering, The University of Tokyo, Hongo, Bunkyo-ku, Tokyo 113-8656, Japan
E-mail: kato@chiral.t.u-tokyo.ac.jp

[b] Japan Synchrotron Radiation Research Institute/SPring-8, 1-1-1 Kouto, Sayo-cho, Sayo-gun, Hyogo 679-5198, Japan

† Electronic supplementary information (ESI) available: Additional optical microscope images and infrared absorption spectra. See DOI: 10.1039/d0cc01950j

Fig. 1 Schematic illustration of possible formation of self-assembled fibers in LC smectic A templates.

This journal is © The Royal Society of Chemistry 2020

at lower temperature and less ordered layered structures of smectic A phases are formed as close to the smectic A-nematic transition temperature. Therefore, self-assembly of gelators in LC smectic A phases was expected to be tuned by thermal conditions due to the temperature-dependent structure of smectic A phases. However, the effects of thermal conditions on molecular self-assembly in LC smectic A templates have not been explored.

Here, we report that new patterned fibrous structures (type III, Fig. 1) are selectively formed through self-assembly of a low-molecular-weight gelator in an LC smectic A template. Anisotropic fiber growth of the gelator in the LC smectic A template is studied at different thermal conditions.

Chemical structures of a gelator and a liquid crystal used in this study are shown in Fig. 2. As a gelator, L-isoleucine-based compound **1** was used because of its significant gelation properties.[44,45] In our previous study, a cyanobiphenyl LC mixture, **MCB**, was used as a smectic A layered template for alignment control of photoluminescent[36] and magneto-active fibers.[39] **MCB** shows nematic and smectic A phases from 80 to 69 °C and from 69 to 17 °C, respectively. The fiber formation temperature of **1** is lower than the isotropic-LC phase transition temperature of **MCB** on cooling, which is of importance for the anisotropic assembly of the gelators.[3]

Fiber formation of the mixture of **MCB** and 1 mol% of **1** was examined at various thermal conditions from 62 to 55 °C on cooling from the isotropic state because the order of layered structures of **MCB** in the smectic A phase should be changed depending on thermal conditions. The mixture of **1**/**MCB** (1.0 mol%) showed an isotropic–nematic and nematic–smectic A phase transitions at 75 and 64 °C on cooling, respectively. Aligned fibers were obtained below 62 °C in the homogenously oriented **MCB** in the smectic A phase (Fig. 3 and S1–S4, ESI†). It should be noted that different alignment morphologies of the fibers were obtained depending on the thermal conditions. Fig. 3 shows optical and scanning electron microscope (SEM) images of the self-assembled fibers formed in the oriented **MCB** template prepared at 62 °C (Fig. 3a) and 59 °C (Fig. 3b) on cooling from the isotropic state at a rate of 5 °C min^{-1}. When the mixture was cooled to 62 °C and applied isothermal annealing for about 10 minutes, the fibers grew only in the
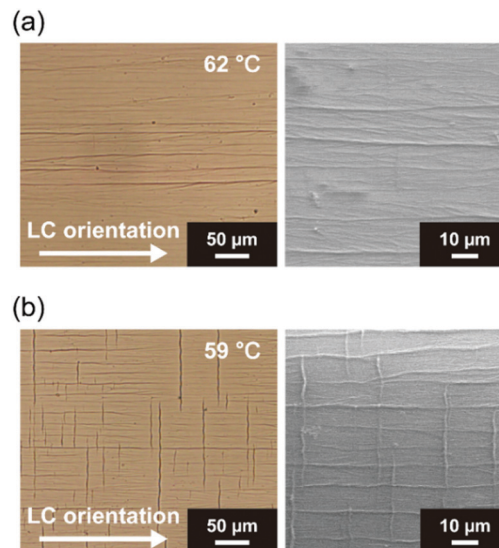

Fig. 3 Optical and scanning electron microscope images of self-assembled fibers of 1 mol% of **1** formed in **MCB** prepared with different annealing temperature at (a) 62 °C and (b) 59 °C after cooling from the isotropic states at 90 °C.

direction parallel to the LC molecular orientation (Fig. 3a). The "type II" fibers covered the all areas after isothermal annealing for about 30 minutes. Dark lines in the optical microscope image at 62 °C are the self-assembled fibers. After removal of the LC molecules, one-directionally oriented fibers were confirmed by SEM observation (type II) (Fig. 3a). Interestingly, when the isothermal annealing temperature of the homogenous LC mixture was lowered below 59 °C, the fibers were formed in both direction parallel and perpendicular to the LC molecular orientation (type III) within 2 minutes (Fig. 3b). An SEM image in Fig. 3b shows a grid-like patterned fibrous structure. The detailed temperature-dependent observations on the anisotropic fiber formation from 62 to 55 °C revealed that the amount of the fibers aligned perpendicular to the LC molecular orientation were increased as the annealing temperature was decreased (Fig. S1, ESI†). These results suggest that the orientation of the self-assembled fibers can be tuned by thermal conditions on the fiber growth in the LC smectic A template. Different concentrations of **1** (0.5, 0.75, 1.5 and 2.0 mol%) in the smectic A phase of **MCB** showed similar tendency in the fiber orientation depending on thermal conditions (Fig. S5 and Table S1, ESI†). Further high concentration of **1** (2.5 mol%) gave spherulitic fibrous aggregates in the nematic phase because the fiber formation occurred above the smectic–nematic phase transition temperature (Fig. S6, ESI†).

The orientation structures of grid-like fibrous assemblies were examined by microscopic polarized infrared (IR) spectroscopy. One-dimensional fibrous assembly was driven by formation of intermolecular hydrogen bonds between amide moieties of **1** (Fig. S7, ESI†).[3,43] The polar plots of the absorbance of the hydrogen-bonded CO (amide) stretching band of **1** at 1646 cm^{-1} for **1**/**MCB** (1.5 mol%) for the grid-like fibrous structure prepared with isothermal annealing at 60 °C are

1

MCB

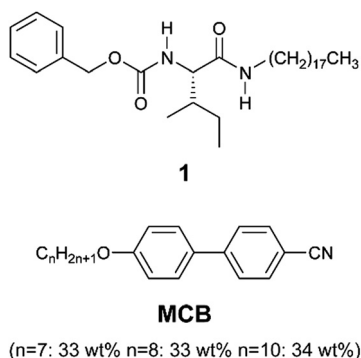(n=7: 33 wt% n=8: 33 wt% n=10: 34 wt%)

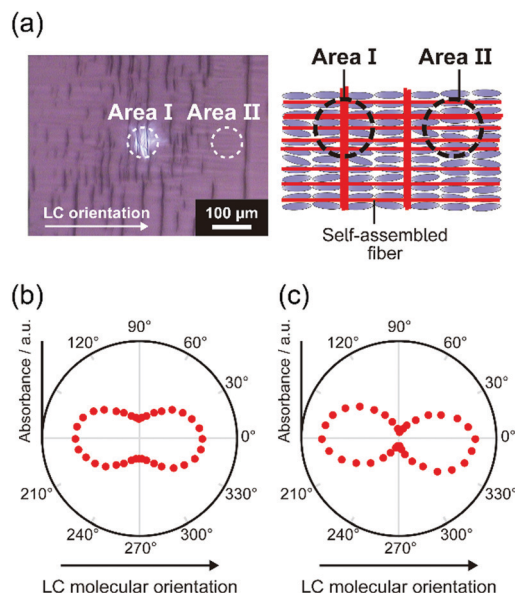Fig. 2 Chemical structures of **1** and **MCB**.

Fig. 4 (a) Optical microscopic image and a schematic illustration of the LC mixture of **1**/**MCB** (1.5 mol%) with the grid-like fibrous structure. Polar plots of the microscopic IR absorbance of the hydrogen-bonded CO (amide) stretching band of **1** for different sampling areas of (b) grid-like (area I) and (c) non-grid-like area (area II).
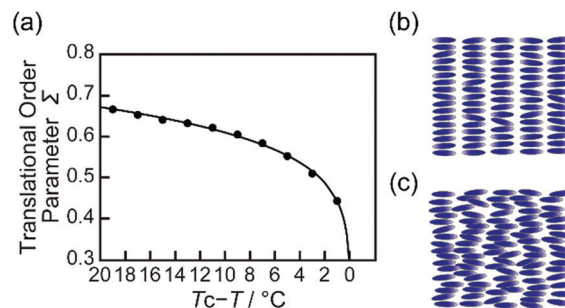

Fig. 5 (a) Temperature-dependent translational order parameter Σ for the smectic A phase of pure **MCB**. Schematic illustrations of a smectic A phase (b) with a more ordered layered structure at lower temperature and (c) with a less ordered layered structure at higher temperature.

shown in Fig. 4. The measurements were conducted at the grid-like (area I) and the non-grid-like fibrous area (area II), where fibers were microscopically aligned in both directions parallel and perpendicular to the LC molecular orientation (area I) and in one direction parallel to the LC molecular orientation (area II). The maximum intensities of the absorbance for CO stretching bands were obtained when the direction of polarized light was parallel to the LC molecular orientation for both areas I and II (Fig. 4 and Fig. S8, ESI†). Dichroic ratio $A_{NH\parallel}/A_{NH\perp}$ for the NH stretching bands for the aligned fibrous assemblies at sampling areas I and II were estimated to be as 3.1 and 10.2, respectively, where $A_{\parallel}$ and $A_{\perp}$ are the absorbance of the band with the infrared light polarization parallel and perpendicular to the LC molecular orientation. The larger dichroic ratio of the NH stretching band for area II corresponds to the macroscopic orientation of the one-directionally aligned fibers. The smaller dichroic ratio for area I is due to the fibers aligned in both direction parallel and perpendicular to the LC molecular orientation. These results also indicate that the fibers were mainly formed along the LC molecular orientation in this mixture.

The translational order parameter Σ and the layer spacing d are important to characterize the layer structure of smectic phase.[43] To examine the order of the LC layered structures, temperature-dependent XRD measurements on the single component of **MCB** in the smectic A phases were performed. The translational order parameter Σ of **MCB** was dependent on temperature (Fig. 5a), while the layer spacing d showed little dependence on temperature (Fig. S9, ESI†). It should be noted that smectic–nematic phase transition temperature T_c depends on the concentration of gelators.[3] Therefore, reduced temperature T_c–T was used. As shown in Fig. 5a, Σ is increased as

decreasing temperature, while Σ was drastically decreased when T_c–T is below around 4 °C. These results suggest that higher regularity of the layered structure is formed at the lower temperature of the smectic A phase (Fig. 5b). When the temperature is close to T_c, the less ordered layered structure was formed (Fig. 5c). For the mixture of **1**/**MCB** (1.0 mol%), T_c–T for 62 and 59 °C are 2 and 5 °C. The mixture of **1**/**MCB** (1.0 mol%) at 59 °C was more ordered layered structure than that at 62 °C. The dependence of orientational order on temperature of the LC molecules of **MCB** in the smectic A phase was also studied by polarized IR measurements (Fig. S10, ESI†).

The proposed mechanism of the formation of the different fiber orientations in the smectic A template is shown in Fig. 6. The fiber morphologies depend on thermal conditions. The mixture of **1**/**MCB** (1 mol%) shows a nematic–smectic A phase transition at 64 °C on cooling from the isotropic state at 90 °C. When the mixture is isothermally annealed at the higher temperature range of the smectic A phase such as 62 °C, a less ordered layered structure is formed, which is suggested by the polarized IR absorption analyses on **MCB**. In the less ordered layered structure of **MCB**, gelator **1** can easily form fibers along the LC molecular orientation. However, the formation of the fibers along the layers is highly disturbed. Therefore, the one-directionally aligned fibrous structures along the LC molecular
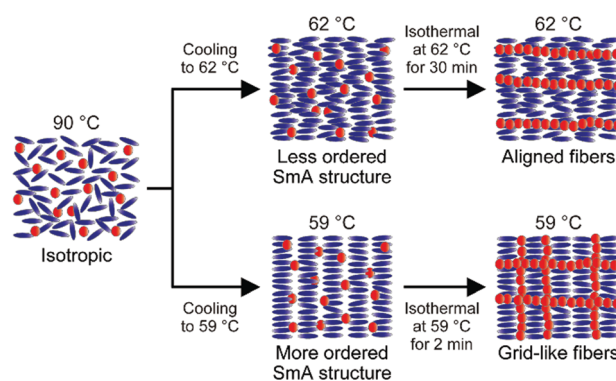

Fig. 6 Schematic illustration of the fiber formation of **1** (1 mol%) in the smectic A (SmA) template of **MCB** depending on different thermal conditions.

orientation are obtained. In contrast, a more ordered layered structure of the smectic A phase is formed by fast cooling to the lower temperature of 59 °C. Owing to the more ordered layered structure of **MCB**, gelator **1** forms fibers not only along the LC molecular orientation but also along the layers, which lead to the formation of the grid-like fibrous structures. For this mixture, no aligned fibers parallel to the layers were not obtained although we kept the mixture at a lower temperature of 25 °C (Fig. S3, ESI†).

In conclusion, grid-type fibrous structures were obtained by using self-assembly of layered LC smectic templates containing low-molecular-weight gelators. In the homogenously oriented LC smectic A phase, aligned fibers in one direction or two orthogonal directions (grid-like structure) were selectively formed depending on thermal conditions. This is the first example of one-step construction of grid-like patterned fibrous structures on microscale through self-assembly processes. Temperature-dependent polarized IR absorption measurements for the LC template suggested that the more ordered layered structure was formed at the lower temperature of the smectic A phase, which promoted fiber growth along the layers. We believe that tuning of the dynamic LC ordered templates is a promising approach to the construction of further complex patterned structures leading to the emergence of novel functions.

Conflicts of interest

There are no conflicts to declare.

Notes and references

1 P. R. A. Chivers and D. K. Smith, *Nat. Rev. Mater.*, 2019, **4**, 463–478.
2 C. D. Jones and J. W. Steed, *Chem. Soc. Rev.*, 2016, **45**, 6546–6596.
3 T. Kato, Y. Hirai, S. Nakaso and M. Moriyama, *Chem. Soc. Rev.*, 2007, **36**, 1857–1867.
4 M. de Loos, B. L. Feringa and J. H. van Esch, *Eur. J. Org. Chem.*, 2005, 3615–3631.
5 C. Stubenrauch and F. Giesselmann, *Angew. Chem., Int. Ed.*, 2016, **55**, 3268–3275.
6 K. Hanabusa and M. Suzuki, *Polym. J.*, 2014, **46**, 776–782.
7 *Low Molecular Mass Gelators*, ed. F. Fages, Springer, Heidelberg, 2005.
8 S. S. Babu, V. K. Praveen and A. Ajayaghosh, *Chem. Rev.*, 2014, **114**, 1973–2129.
9 T. Kato and K. Tanabe, *Chem. Lett.*, 2009, **38**, 634–639.
10 D. A. Stone, A. S. Tayi, J. E. Goldberger, L. C. Palmer and S. I. Stupp, *Chem. Commun.*, 2011, **47**, 5702–5704.
11 G. A. Silva, C. Czeisler, K. L. Niece, E. Beniash, D. A. Harrington, J. A. Kessler and S. I. Stupp, *Science*, 2004, **303**, 1352–1355.
12 S. Kiyonaka, K. Sada, I. Yoshimura, S. Shinkai, N. Kato and I. Hamachi, *Nat. Mater.*, 2004, **3**, 58–64.
13 P. Xing and Y. Zhao, *Acc. Chem. Res.*, 2018, **51**, 2324–2334.
14 D. Yamaguchi, H. Eimura, M. Yoshio and T. Kato, *Chem. Lett.*, 2016, **45**, 863–865.
15 F. Tantakitti, J. Boekhoven, X. Wang, R. V. Kazantsev, T. Yu, J. Li, E. Zhuang, R. Zandi, J. H. Ortony, C. J. Newcomb, L. C. Palmer, G. S. Shekhawat, M. O. de la Cruz, G. C. Schatz and S. I. Stupp, *Nat. Mater.*, 2016, **15**, 469–476.
16 K. Fukushima, J. P. K. Tan, P. A. Korevaar, Y. Y. Yang, J. Pitera, A. Nelson, H. Maune, D. J. Coady, J. E. Frommer, A. C. Engler, Y. Huang, K. Xu, Z. Ji, Y. Qiao, W. Fan, L. Li, N. Wiradharma, E. W. Meijer and J. L. Hedrick, *ACS Nano*, 2012, **10**, 9191–9199.
17 D. J. Welsh, P. Posocco, S. Pricl and D. K. Smith, *Org. Biomol. Chem.*, 2013, **11**, 3177–3186.
18 M. Lescanne, A. Colin, O. Mondain-Monvel, F. Fages and J.-L. Pozzo, *Langmuir*, 2003, **19**, 2013–2020.
19 X. Huang, P. Terech, S. R. Raghavan and R. G. Weiss, *J. Am. Chem. Soc.*, 2005, **127**, 4336–4344.
20 N. Mizoshita, K. Hanabusa and T. Kato, *Adv. Funct. Mater.*, 2003, **13**, 313–317.
21 Y. Suzuki, N. Mizoshita, K. Kishimoto, K. Hanabusda and T. Kato, *J. Mater. Chem.*, 2003, **13**, 2870–2874.
22 L. Guan and Y. Zhao, *J. Mater. Chem.*, 2001, **11**, 1339–1344.
23 B. Su, Y. Wu and L. Jiang, *Chem. Soc. Rev.*, 2012, **41**, 7832–7856.
24 L. Sardone, V. Palermo, E. Devaux, D. Credgington, M. de Loos, G. Marletta, F. Cacialli, J. van Esch and P. Samorì, *Adv. Mater.*, 2006, **18**, 1276–1280.
25 Y. Shoji, M. Yoshio, T. Yasuda, M. Funahashi and T. Kato, *J. Mater. Chem.*, 2010, **20**, 173–179.
26 I. O. Shklyarevskiy, P. Jonkheijm, P. C. M. Christianen, A. P. H. J. Schenning, A. D. Guerzo, J.-P. Desvergne, E. W. Meijer and J. C. Maan, *Langmuir*, 2005, **21**, 2108–2112.
27 P. van der Asdonk, M. Keshavarz, P. C. M. Christianen and P. H. J. Kouwer, *Soft Matter*, 2016, **12**, 6518–6525.
28 K. Yabuuchi and T. Kato, in *Handbook of Liquid Crystals*, ed. J. W. Goodby, P. J. Collings, T. Kato, C. Tschierske, H. F. Gleeson and P. Raynes, Wiley-VCH, Weinheim, 2nd edn, 2014, vol. 6, pp. 1–25.
29 T. Kitamura, S. Nakaso, N. Mizoshita, Y. Tochigi, T. Shimomura, M. Moriyama, K. Ito and T. Kato, *J. Am. Chem. Soc.*, 2005, **127**, 14769–14775.
30 N. Mizoshita and T. Kato, *Adv. Funct. Mater.*, 2006, **16**, 2218–2224.
31 M. Goh, S. Matsushita and K. Akagi, *Chem. Soc. Rev.*, 2010, **39**, 2466–2476.
32 K. C. K. Cheng, M. A. B. Pantoja, Y.-K. Kim, J. V. Gregory, F. Xie, A. de France, C. Hussal, K. Sun, N. L. Abbott and J. Lahann, *Science*, 2018, **362**, 804–808.
33 P. van der Asdonk and P. H. J. Kouwer, *Chem. Soc. Rev.*, 2017, **46**, 5935–5949.
34 N. Mizoshita, T. Kutsuna, K. Hanabusa and T. Kato, *Chem. Commun.*, 1999, 781–782.
35 J. F. Hulvat and S. I. Stupp, *Adv. Mater.*, 2004, **16**, 589–592.
36 Y. Hirai, S. S. Babu, V. K. Praveen, T. Yasuda, A. Ajayaghosh and T. Kato, *Adv. Mater.*, 2009, **21**, 4029–4033.
37 N. B. Topani, N. Prutha and R. Pratibha, *ChemPhysChem*, 2018, **19**, 1471–1475.
38 K. Yabuuchi, Y. Tochigi, N. Mizoshita, K. Hanabusa and T. Kato, *Tetrahedron*, 2007, **63**, 7358–7365.
39 H. Eimura, Y. Umeta, H. Tokoro, M. Yoshio, S. Ohkoshi and T. Kato, *Chem. – Eur. J.*, 2016, **22**, 8872–8878.
40 X. Wang, D. S. Miller, E. Bukusoglu, J. J. de Pablo and N. L. Abbott, *Nat. Mater.*, 2016, **15**, 106–112.
41 B. Bhattacharjee, S. Paul and R. Paul, *Mol. Cryst. Liq. Cryst.*, 1982, **89**, 181–192.
42 M. K. Das, S. Paul and R. Paul, *Mol. Cryst. Liq. Cryst.*, 1995, **264**, 89–98.
43 N. Kapernaum and F. Giesselmann, *Phys. Rev. E: Stat., Nonlinear, Soft Matter Phys.*, 2008, **78**, 062701.
44 K. Hanabusa, K. Hiratsuka, M. Kimura and H. Shirai, *Chem. Mater.*, 1999, **11**, 649–655.
45 N. Mizoshita, K. Hanabusa and T. Kato, *Adv. Mater.*, 1999, **11**, 392–394.